Study of quasi-projectile breakup in semiperipheral collisions of ^{64,58}Ni+^{64,58}Ni at 32 *A*MeV and 52 *A*MeV with the INDRA-FAZIA apparatus

Caterina Ciampi,
INFN and University of Florence

for the INDRA-FAZIA collaboration

XXII colloque GANIL
September 26th - October 1st 2021

Contents

- Introduction:
  - the INDRA-FAZIA apparatus
  - the E789 experiment
  - a brief description of the QP breakup channel
- Selection of the reaction channels
  - **QPr**: QP evaporation
  - **QPb**: QP breakup
- Isospin equilibration in the two selected reaction channels
- Conclusions and future perspectives

INDRA-FAZIA

The experimental apparatus

INDRA and FAZIA: multi-detector apparatuses, designed for the detection of nuclear fragments produced in heavy ion collisions at Fermi energies.

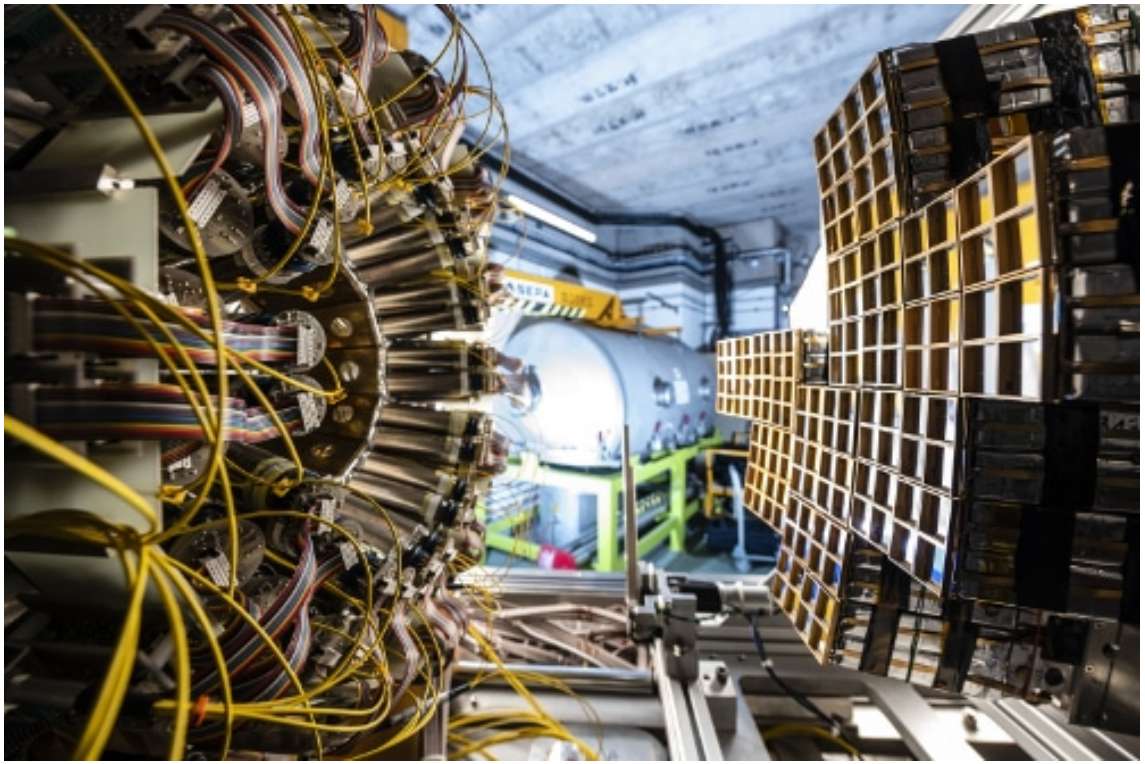

[95pou, 14bou, 19val]

During the first months of 2019, the coupling between INDRA (rings 6 to 17) and FAZIA (12 blocks) was completed in GANIL.

The complete setup allows to exploit both the large angular coverage of the INDRA apparatus and the optimal (Z, A) identification provided by FAZIA at forward angles, for QP-like fragments.

The E789 experiment

New insights on the symmetry energy term of the Nuclear Equation of State

The E789 experiment (april-may 2019) is the first campaign to exploit the coupled INDRA-FAZIA apparatus:

- All of the four possible combinations of the two reaction partners ^{58}Ni and ^{64}Ni have been studied
  $\Rightarrow$ compare the products of the two asymmetric reactions with those of both the neutron rich and neutron deficient symmetric systems
- Two different incident beam energies 32 AMeV and 52 AMeV
  $\Rightarrow$ different timescale of the interaction process and different inspected nuclear density range

The aim is to investigate the very active subject of the symmetry energy term of the Nuclear Equation of State [13li, 21ree], by studying the isospin transport phenomena:

- isospin equilibration between QP and QT in semiperipheral collisions (binary output channel) in asymmetric reactions $\rightarrow$ isospin diffusion
- neutron enrichment in the neck region $\rightarrow$ isospin drift

$\rightarrow$ A comparison with AMD+GEMINI++ simulations (filtered according to the actual apparatus acceptance) will be presented in the following

The E789 experiment

Breakup of the QP

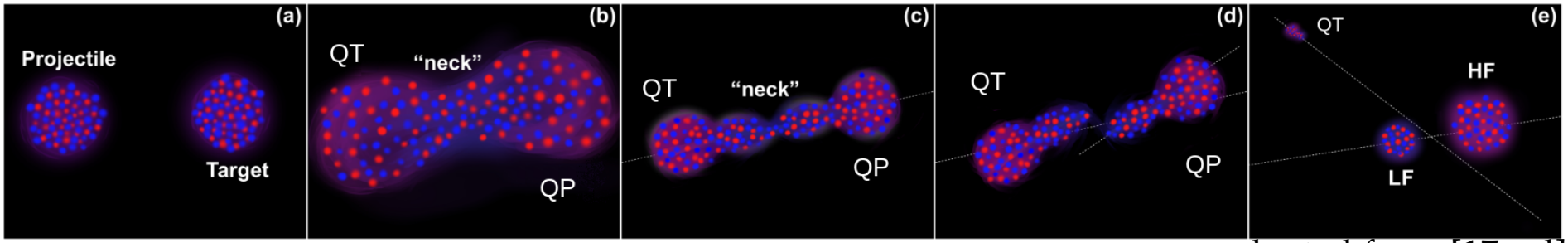

adapted from [17rod]

In the present work we extend the study to an additional reaction channel, i.e. the **breakup or dynamical fission**: **fast, asymmetric and anisotropic** fission process, with a time scale of the order of $200 - 300$ fm/c: [95ste, 93cas, 00boc, 20pia]

- different from the statistical fission, which is a de-excitation process competing with the evaporation, characterised by a longer time scale and an isotropic angular emission
- after their separation, the QP and QT can feature a strong deformation → the deformation can lead to a subsequent prompt breakup
- the observation of an IMF ($Z = 3, 4$) in the midvelocity region can be interpreted as the most asymmetric case of QP (or QT) breakup
- the isospin equilibration can be also studied between the two breakup fragments (HF, LF) [17jed, 17rod]

The E789 experiment

Acquired data

Energy	Projectile	Target	b_{gr} (fm)	$\theta_{gr}^{\mathrm{lab}}$ (deg)	v_{CM}^{lab} (mm/ns)	v_{beam}^{lab} (mm/ns)	v_{beam}^{CM} (mm/ns)
32 AMeV	^{58}Ni	^{58}Ni	10.6	3.3	39.3	78.6	39.3
		^{64}Ni	10.8	3.2	37.4	78.6	41.2
	^{64}Ni	^{58}Ni	10.8	2.9	41.2	78.6	37.4
		^{64}Ni	11.1	2.9	39.3	78.6	39.3
52 AMeV	^{58}Ni	^{58}Ni	10.9	2.0	50.1	100.2	50.1
		^{64}Ni	11.1	1.9	47.6	100.2	52.6
	^{64}Ni	^{58}Ni	11.1	1.8	52.6	100.2	47.6
		^{64}Ni	11.3	1.7	50.1	100.2	50.1

A total of about $30 \cdot 10^6$ events was acquired for each measured reactions

- identification procedures completed
- calibration procedures completed for FAZIA and INDRA rings up to 9

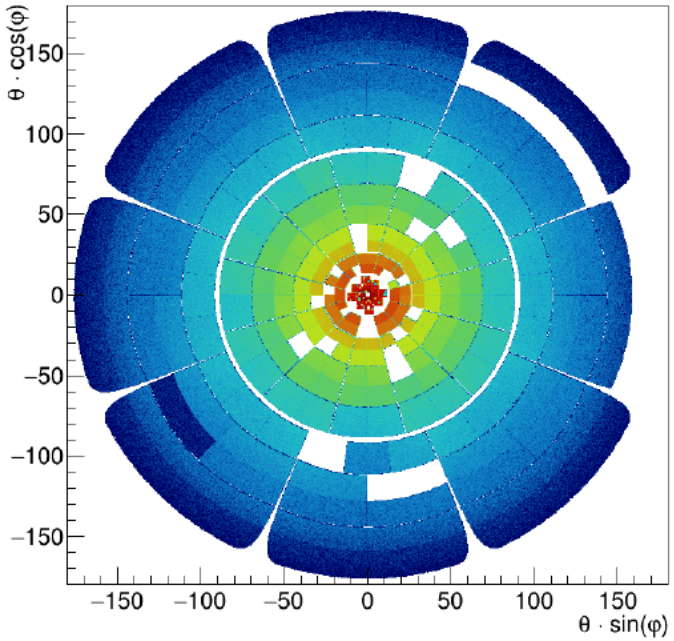

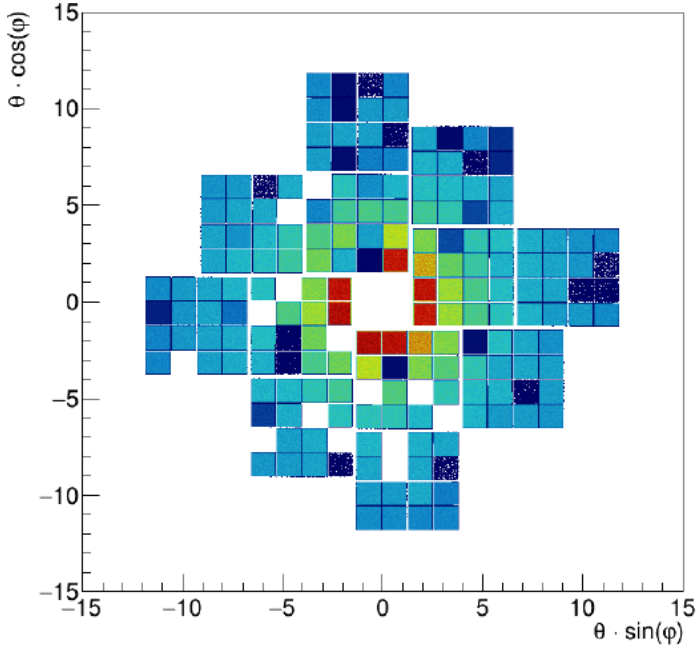

Selection of the reaction channels

QPr: QP evaporation channel

QP remnant: $\mathbf{M_{big} = 1}$, with $Z_{big} \geq 15$ and $\theta_{big}^{CM} < 90°(v_z^{CM} > 0)$

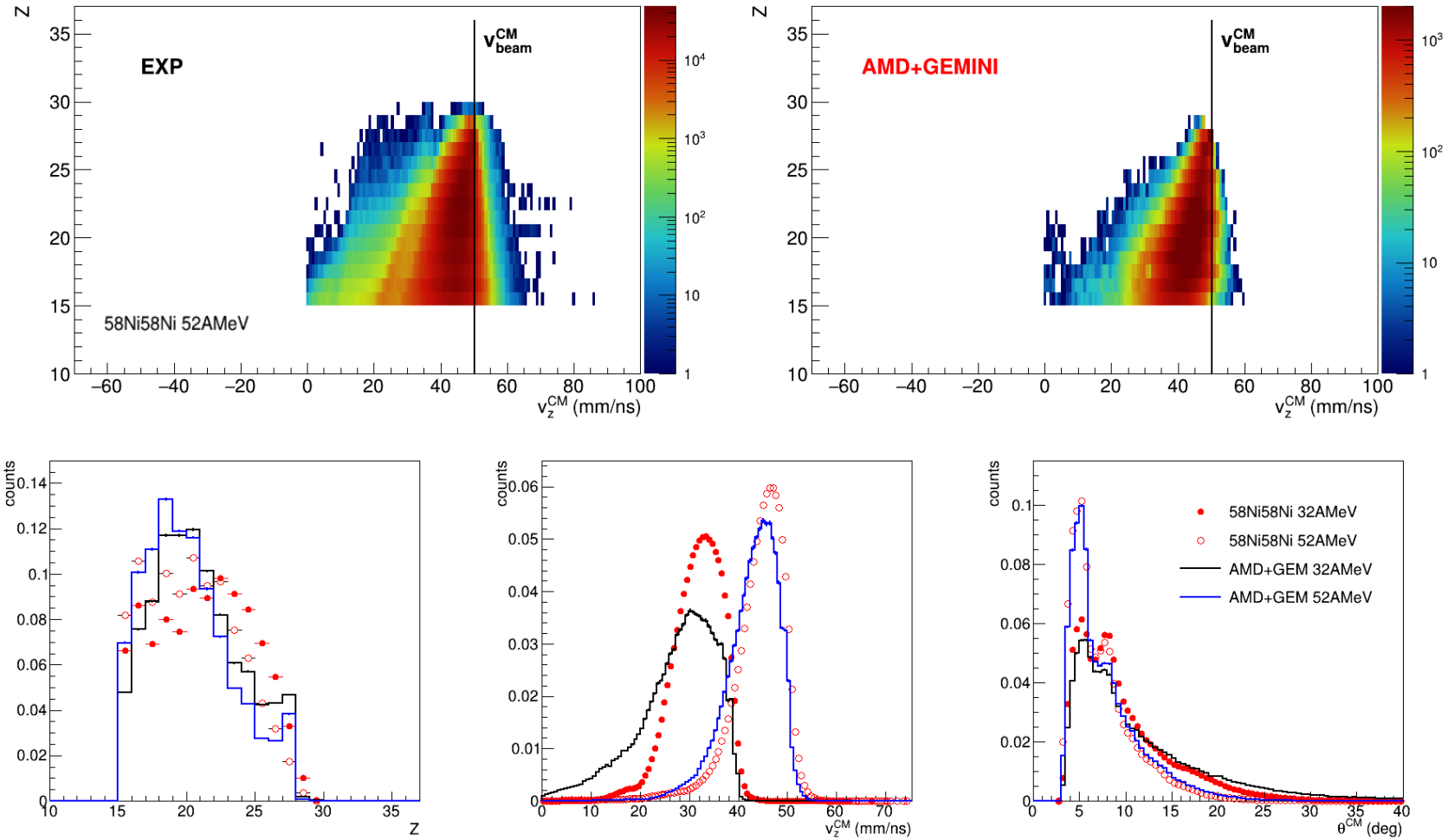

Selection of the reaction channels

QPb: QP breakup channel selection

QP breakup: events with $\mathbf{M_{big} = 2}$

Selection of the reaction channels

QPb: QP breakup channel selection

QP breakup: events with $\mathbf{M_{big} = 2}$

- binary events where both the QP and (a fragment of) the QT are detected,

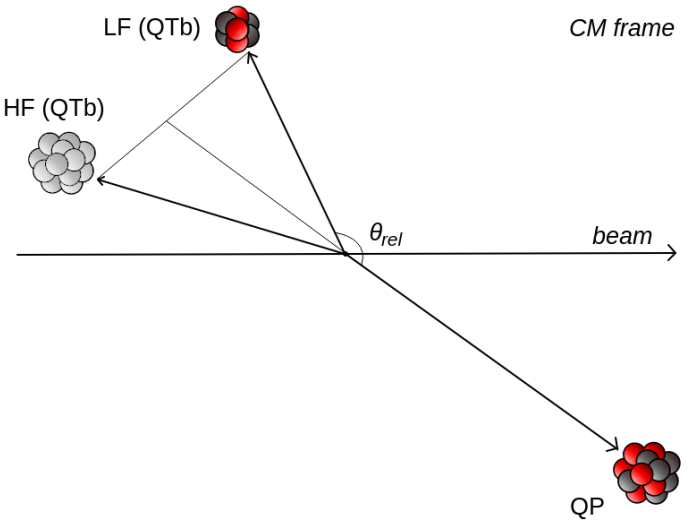

Selection of the reaction channels

QPb: QP breakup channel selection

QP breakup: events with $\mathbf{M_{big} = 2}$

- binary events where both the QP and (a fragment of) the QT are detected, *or QP breakup event (QT not detected)*

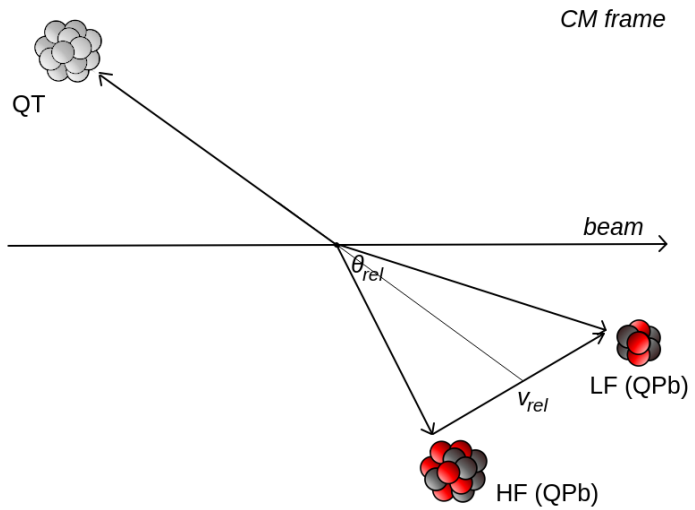

Selection of the reaction channels

QPb: QP breakup channel selection

QP breakup: events with $\mathbf{M_{big} = 2}$

- binary events where both the QP and (a fragment of) the QT are detected, *or QP breakup event (QT not detected)*
- we separate the two kinds of $M_{big} = 2$ events by studying the correlation of the angle between the directions of the two fragments (in the CM) θ_{rel} and their relative velocity v_{rel}

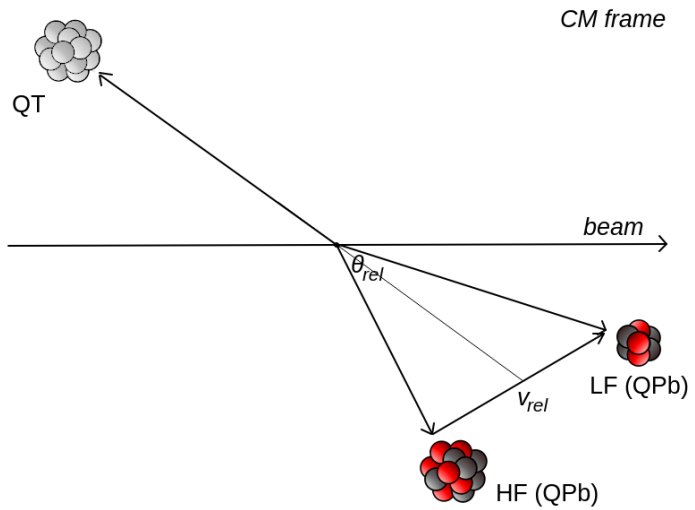

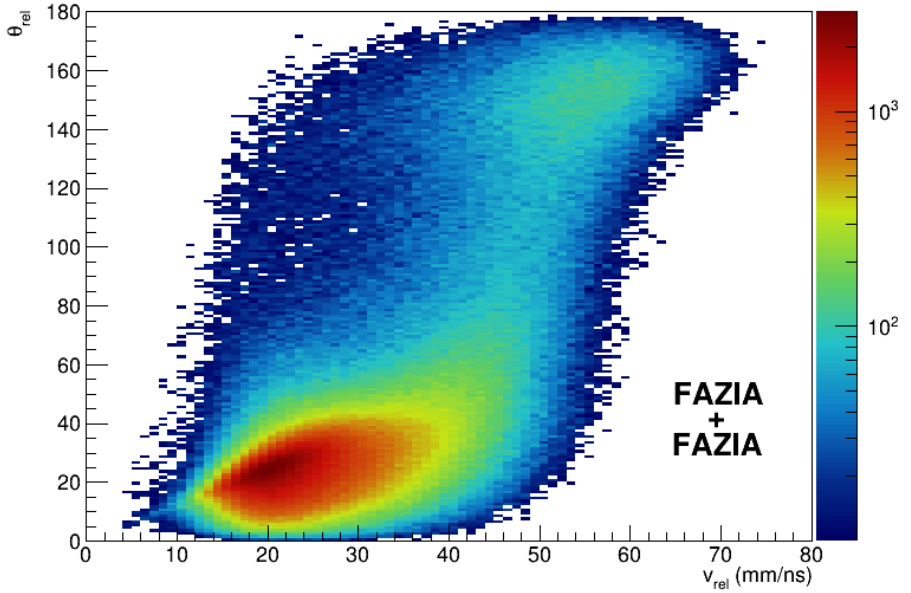

Selection of the reaction channels

QPb: QP breakup channel selection

QP breakup: events with $\mathbf{M_{big} = 2}$

- binary events where both the QP and (a fragment of) the QT are detected, *or QP breakup event (QT not detected)*
- we separate the two kinds of $M_{big} = 2$ events by studying the correlation of the angle between the directions of the two fragments (in the CM) θ_{rel} and their relative velocity v_{rel}
  - $\theta_{rel} > 120°$: QP+QT

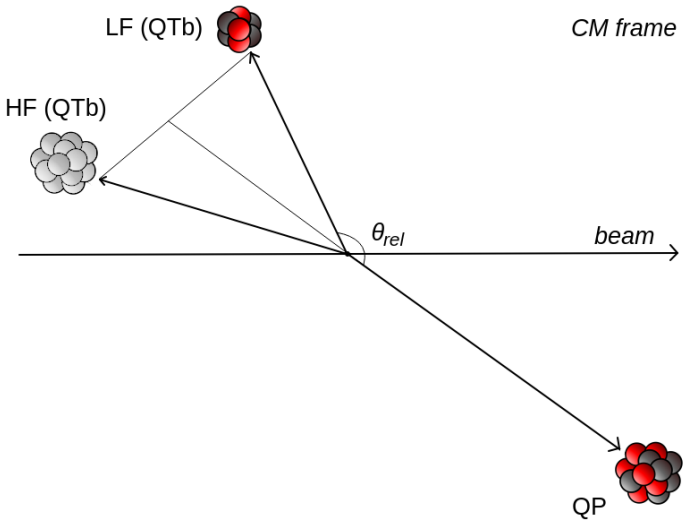

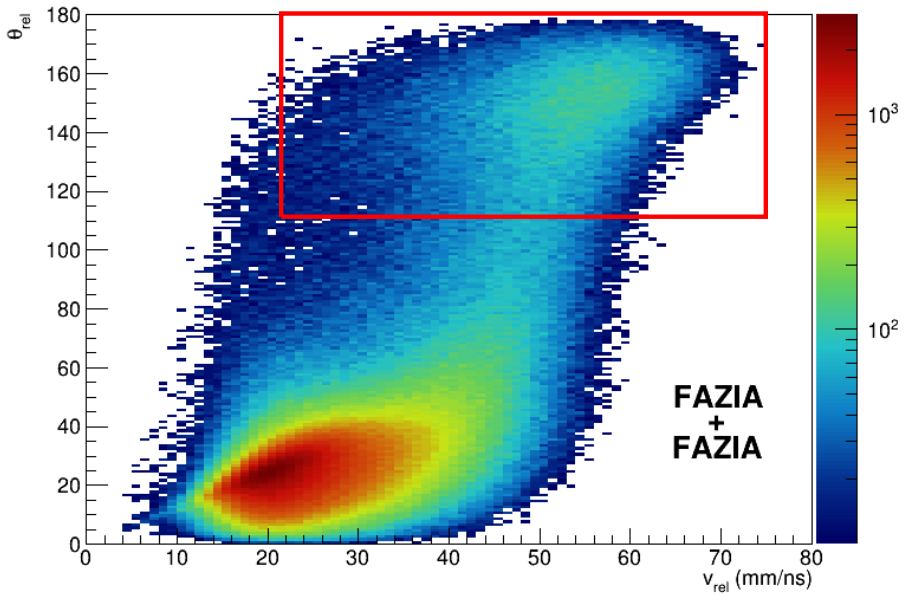

Selection of the reaction channels

QPb: QP breakup channel selection

QP breakup: events with $\mathbf{M_{big} = 2}$

- binary events where both the QP and (a fragment of) the QT are detected, *or* *QP breakup event (QT not detected)*
- we separate the two kinds of $M_{big} = 2$ events by studying the correlation of the angle between the directions of the two fragments (in the CM) θ_{rel} and their relative velocity v_{rel}
  - $\theta_{rel} > 120°$: QP+QT
  - $\theta_{rel} < 90°$: QP breakup

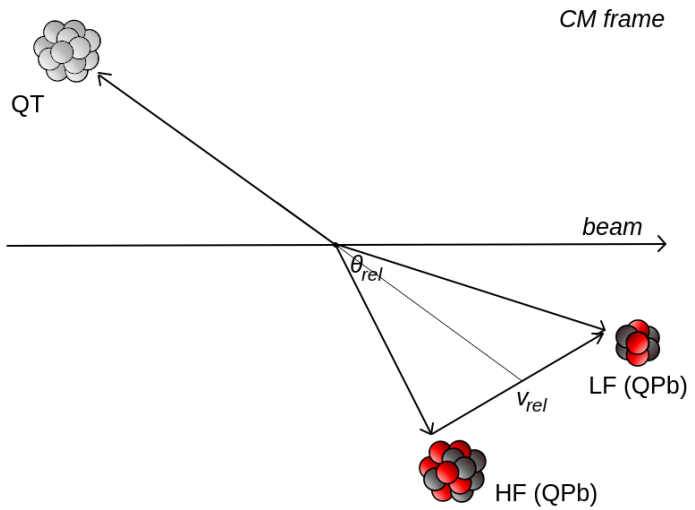

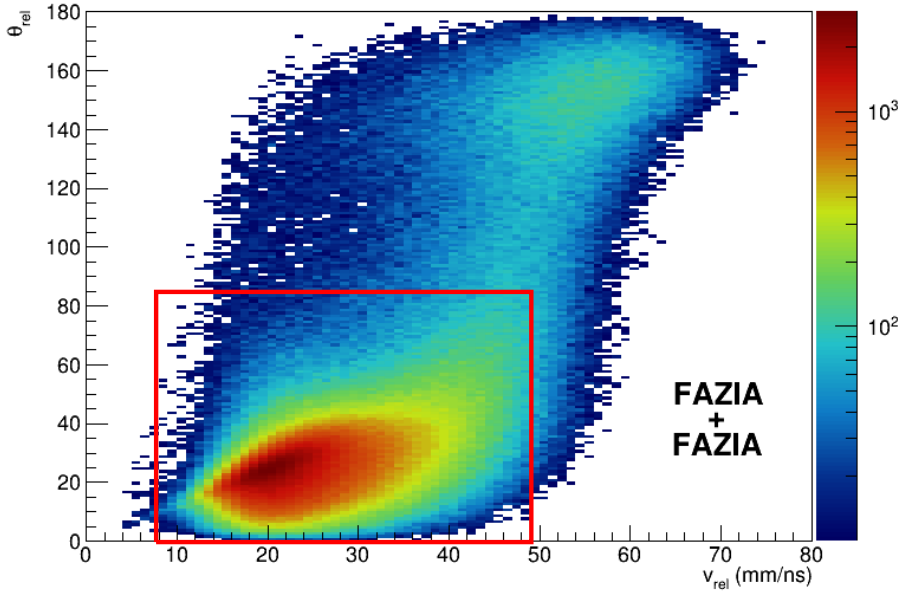

Selection of the reaction channels

QPb: QP breakup channel selection

QP breakup: events with $\mathbf{M_{big} = 2}$

- binary events where both the QP and (a fragment of) the QT are detected, *or QP breakup event (QT not detected)*
- we separate the two kinds of $M_{big} = 2$ events by studying the correlation of the angle between the directions of the two fragments (in the CM) θ_{rel} and their relative velocity v_{rel}
  - $\theta_{rel} > 120°$: QP+QT
  - $\theta_{rel} < 90°$: QP breakup
  - conditions also on the v_{rel} depending on the reaction energy, and on $Z_H + Z_L \geq 15$

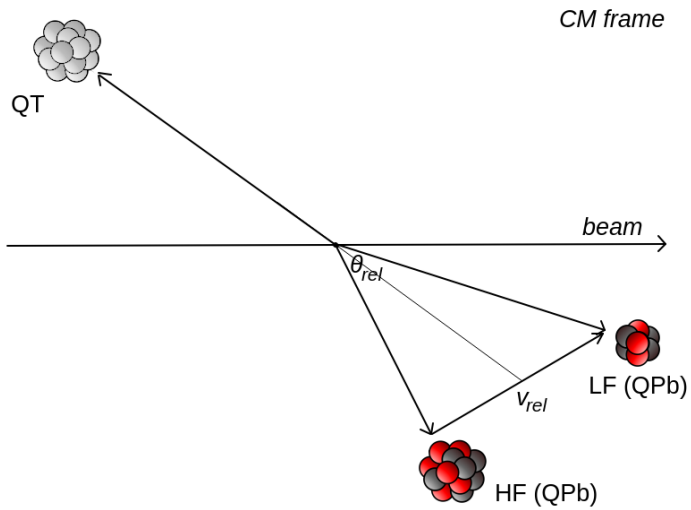

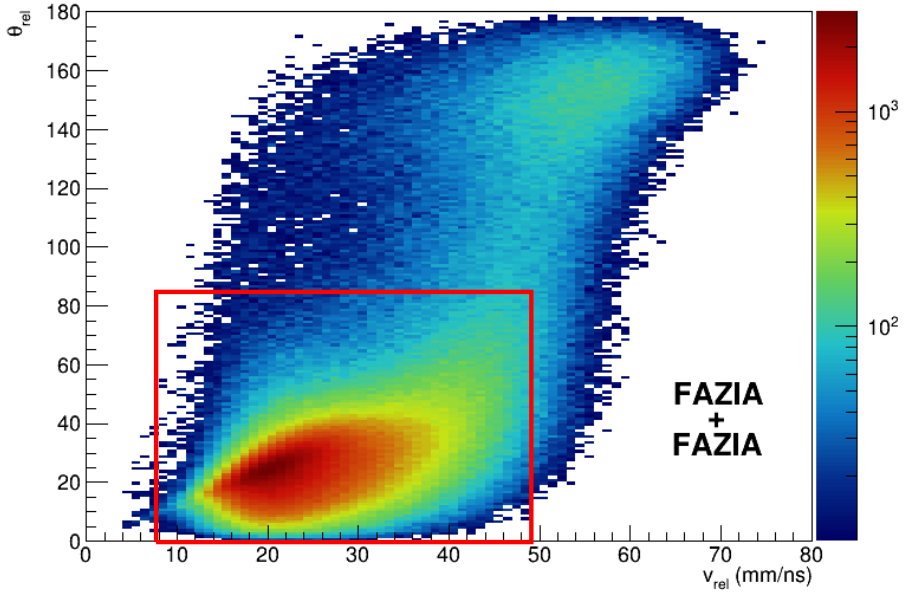

Selection of the reaction channels

QPb: QP breakup channel characteristics (I)

Z vs v^{CM} of the two breakup fragments and of the reconstructed QP:

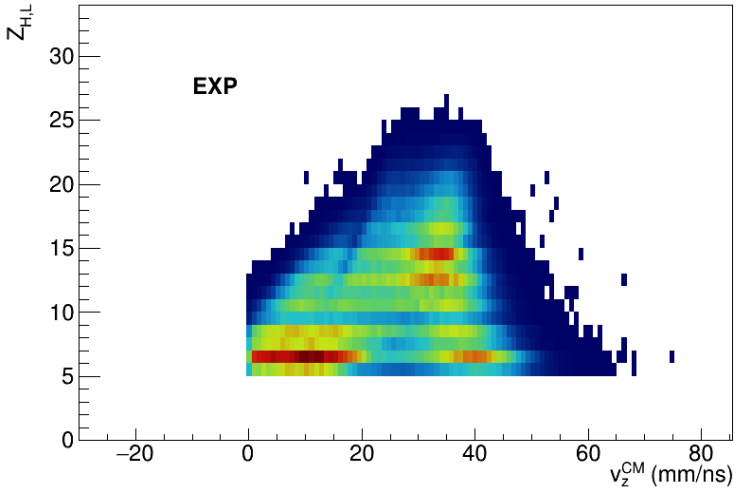

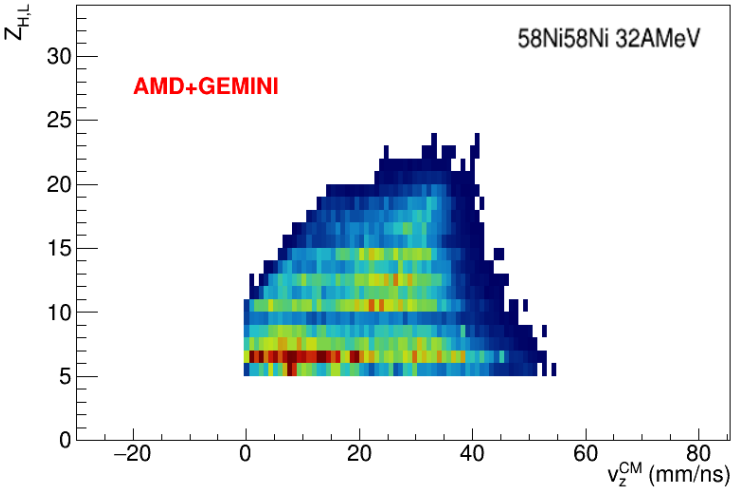

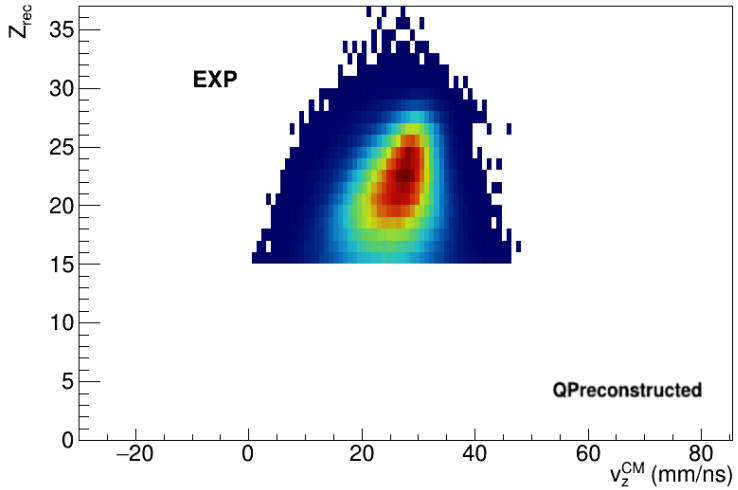

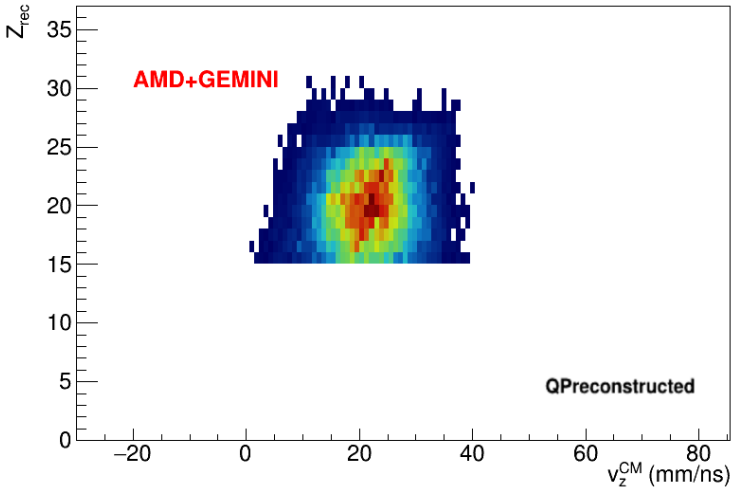

Selection of the reaction channels

QPb: QP breakup channel characteristics (I)

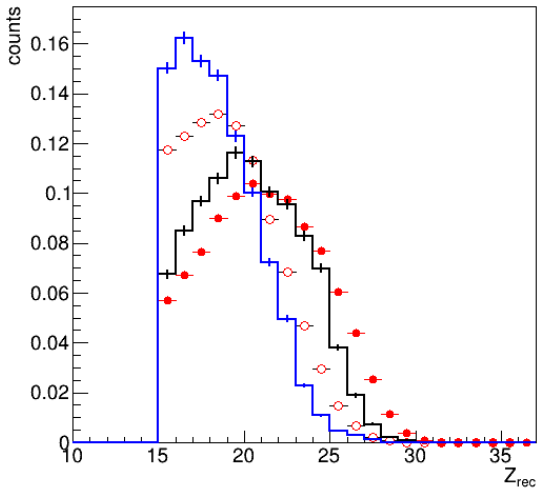

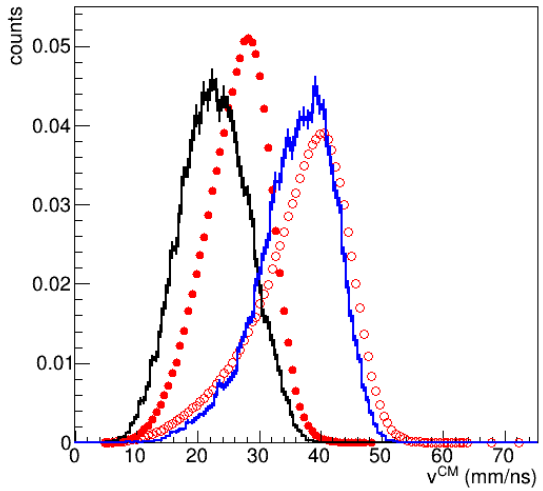

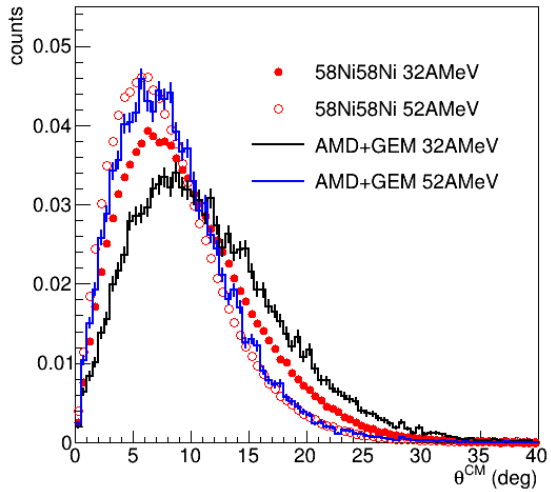

Characteristics of the reconstructed QP:

- Z, v^{CM} and θ^{CM} distributions show a good agreement between experimental data and AMD+GEMINI++ simulations
- Same selection $\rightarrow$ slightly more dissipative collisions in the simulated events than in the experimental ones

Selection of the reaction channels

QPb: QP breakup channel characteristics (I)

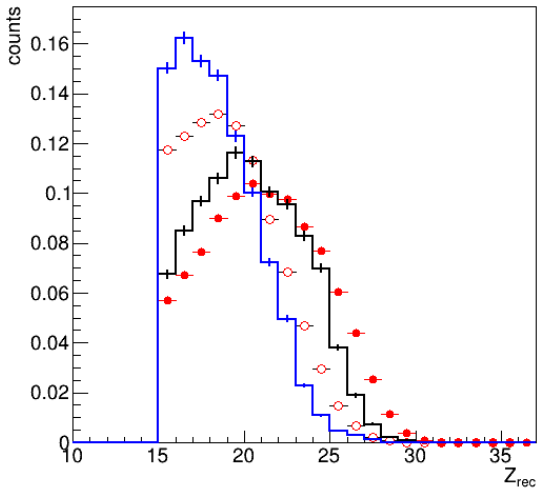

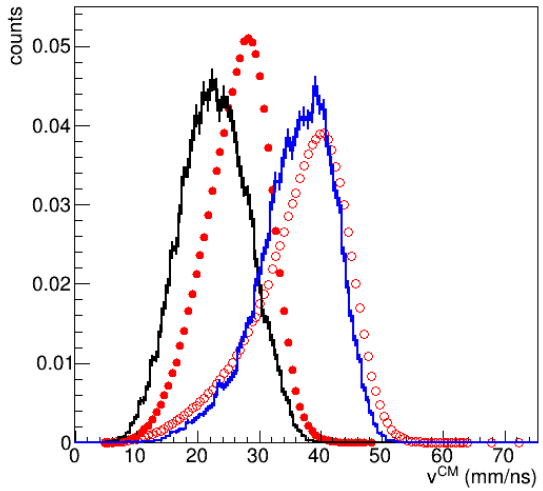

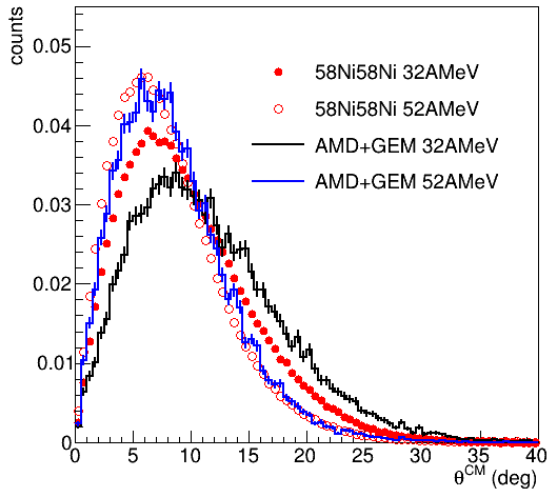

Characteristics of the reconstructed QP:

- Z, v^{CM} and θ^{CM} distributions show a good agreement between experimental data and AMD+GEMINI++ simulations
- Same selection $\rightarrow$ slightly more dissipative collisions in the simulated events than in the experimental ones

We can also study the characteristics of the two breakup fragments...

Selection of the reaction channels

QPb: QP breakup channel characteristics (II)

Charge asymmetry between H and L:

$$\eta = \frac{Z_H - Z_L}{Z_{rec}}$$

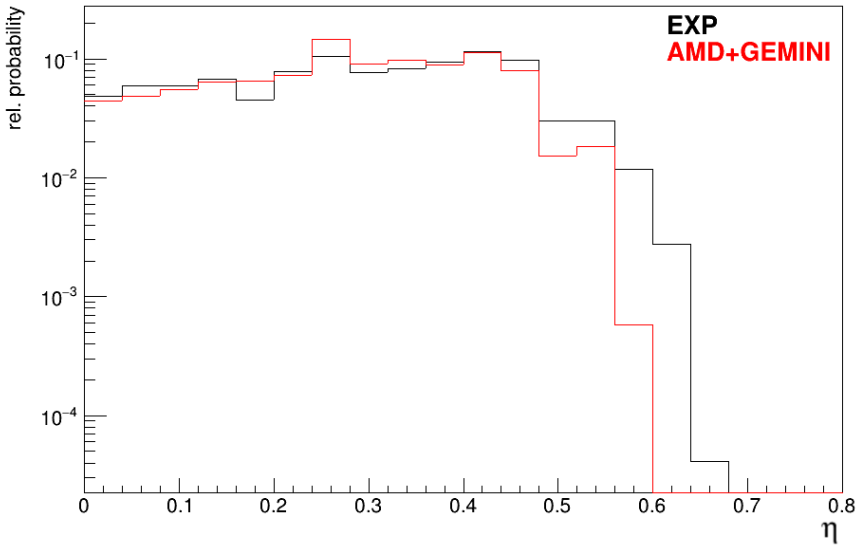

Selection of the reaction channels

QPb: QP breakup channel characteristics (II)

Charge asymmetry between H and L:

$$\eta = \frac{Z_H - Z_L}{Z_{rec}}$$

- three η intervals:
  - $\eta \leq 0.2 \rightarrow$ symmetric
  - $0.2 < \eta \leq 0.4$
  - $0.4 < \eta \leq 0.6 \rightarrow$ asymmetric

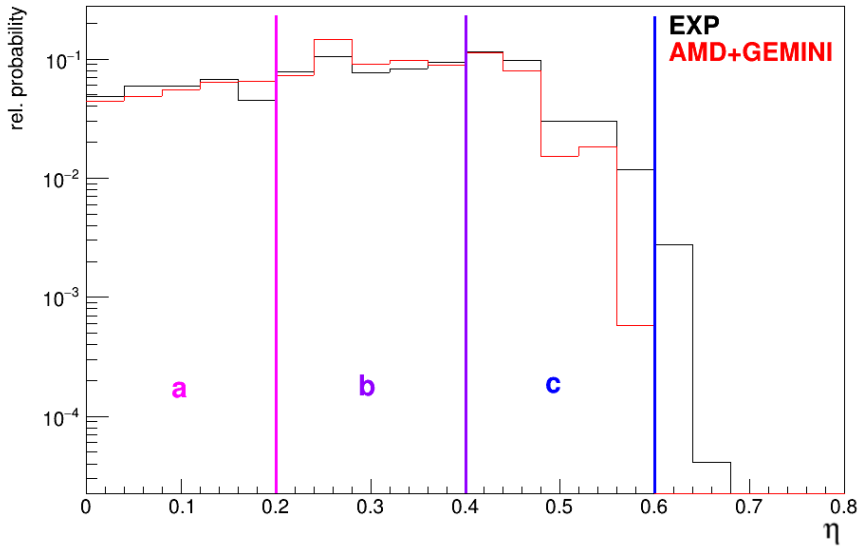

Selection of the reaction channels

QPb: QP breakup channel characteristics (II)

Charge asymmetry between H and L:

$$\eta = \frac{Z_H - Z_L}{Z_{rec}}$$

- three η intervals:
  - $\eta \leq 0.2 \rightarrow$ symmetric
  - $0.2 < \eta \leq 0.4$
  - $0.4 < \eta \leq 0.6 \rightarrow$ asymmetric

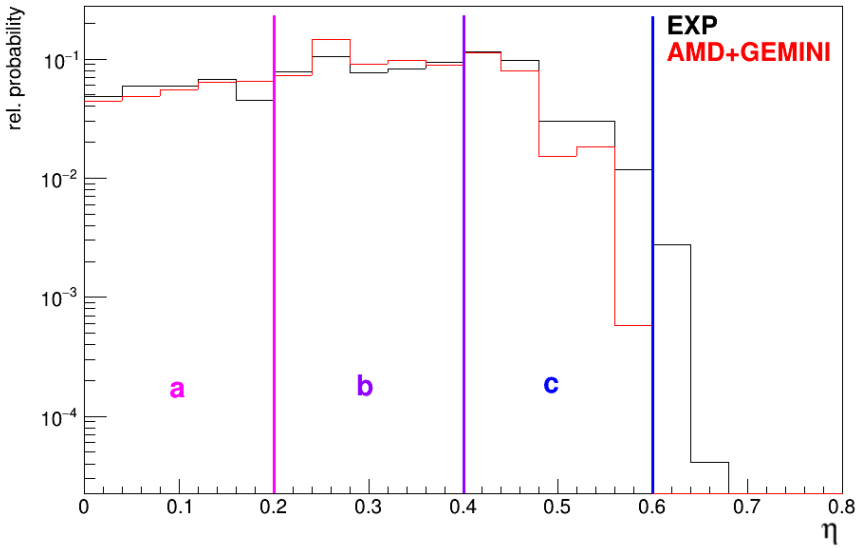

α angle between the QP-QT separation axis ($\vec{v}_{QP_{rec}}$) and the breakup axis ($\vec{v}_{rel}$):

- in the asymmetric configuration the backward emission of the LF is favoured, as expected

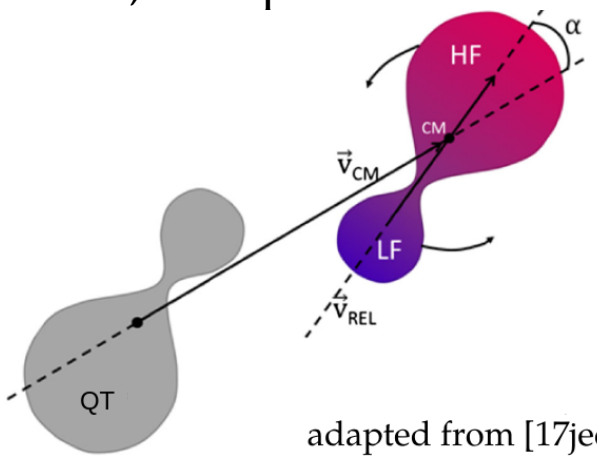

adapted from [17jed]

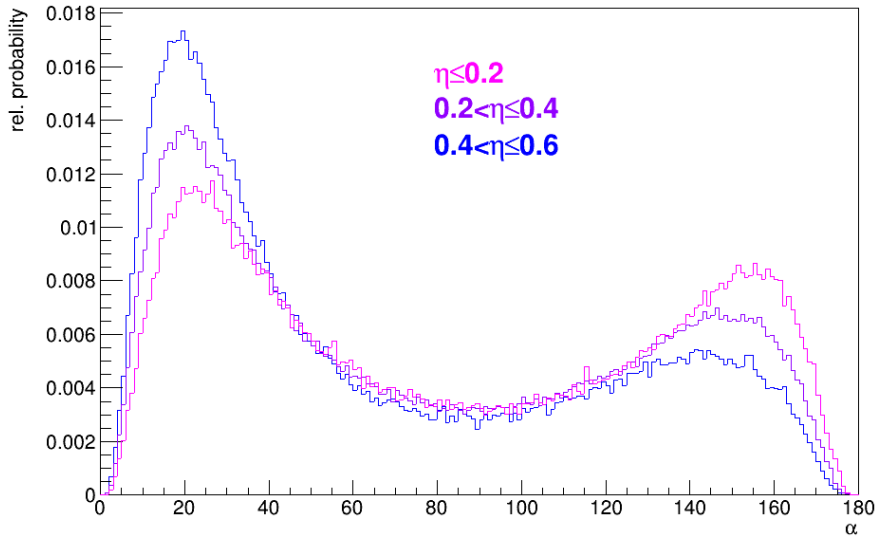

Reaction centrality estimation

Reduced QP momentum along the beam axis p_{red}

Reduced momentum along the z-axis:

$$p_{red} = \frac{p_z^{QP}}{p_{beam}}$$

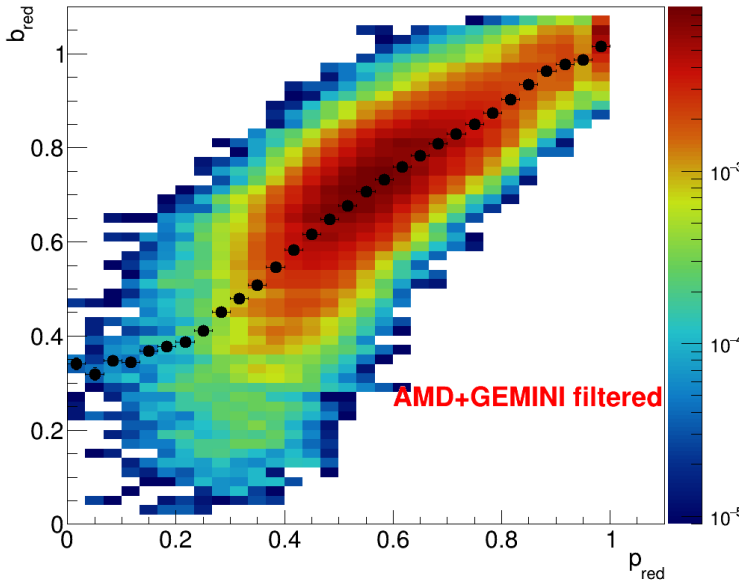

Reaction centrality estimation

Reduced QP momentum along the beam axis p_{red}

Reduced momentum along the z-axis:

$$p_{red} = \frac{p_z^{QP}}{p_{beam}}$$

- realiable for $p_{red} \gtrsim 0.3$
- its correlation with $b_{red} = b/b_{gr}$ is similar among the different reactions

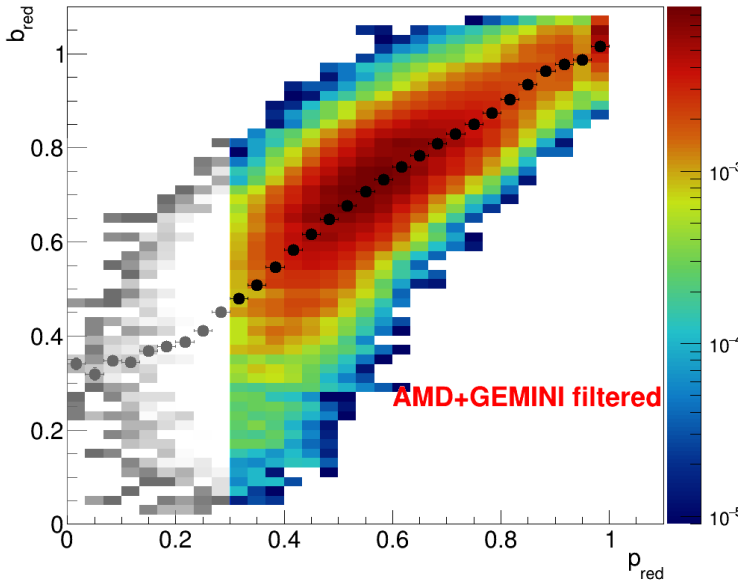

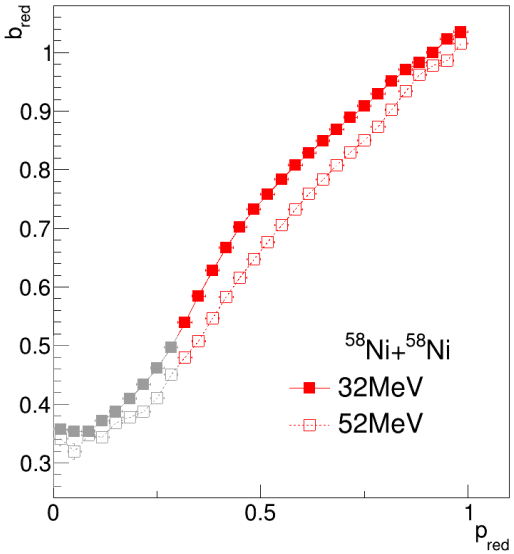

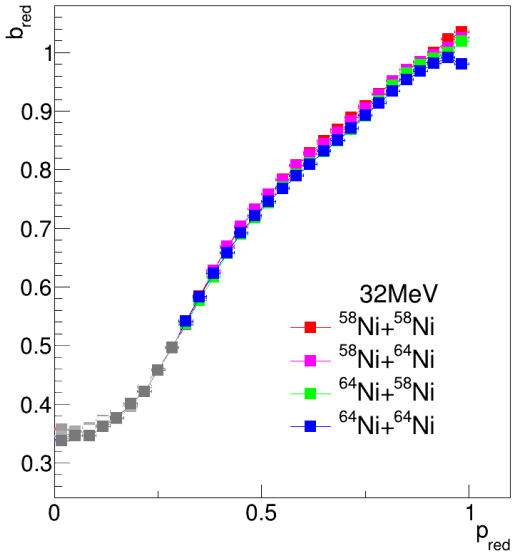

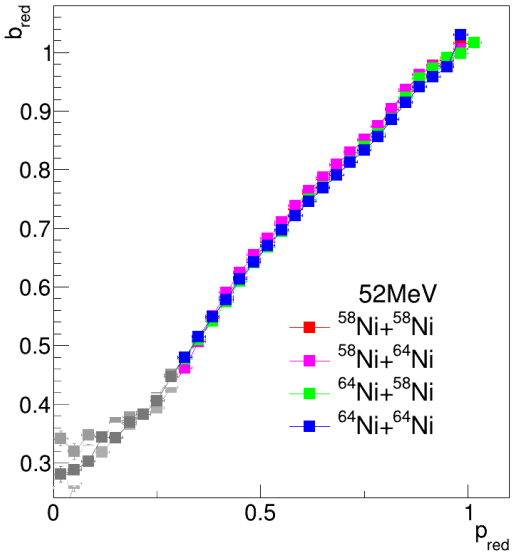

Reaction centrality estimation

Reduced QP momentum along the beam axis p_{red}

Reduced momentum along the z-axis:

$$p_{red} = \frac{p_z^{QP}}{p_{beam}}$$

- realiable for $p_{red} \gtrsim 0.3$
- its correlation with $b_{red} = b/b_{gr}$ is similar among the different reactions and between the two selected reaction channels

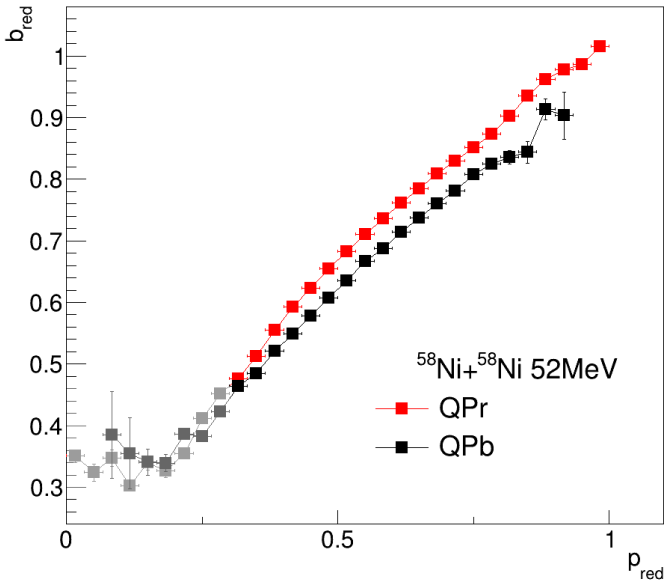

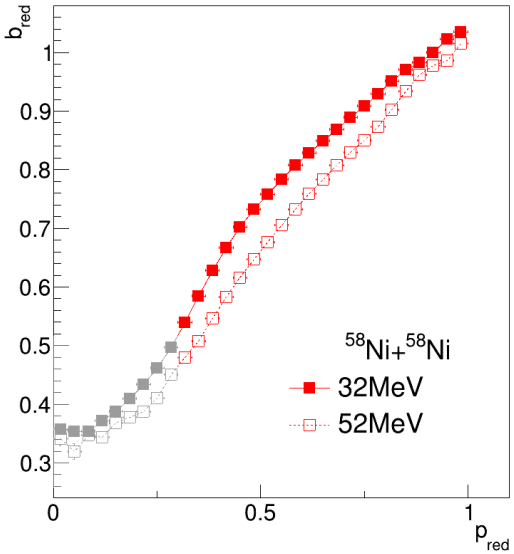

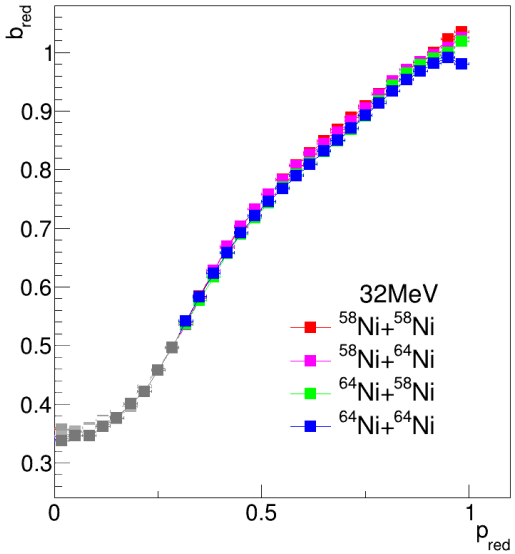

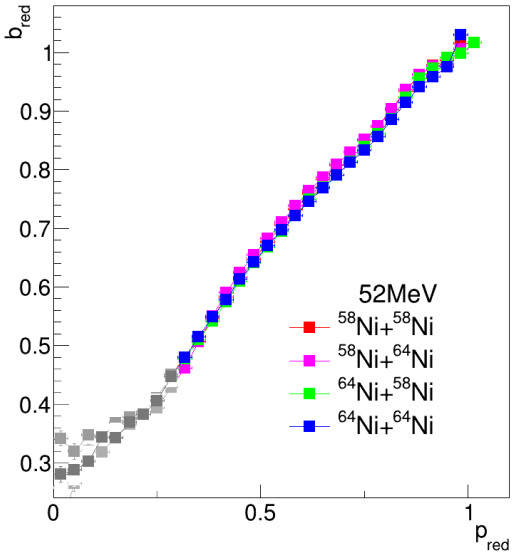

Isospin equilibration

QPr channel

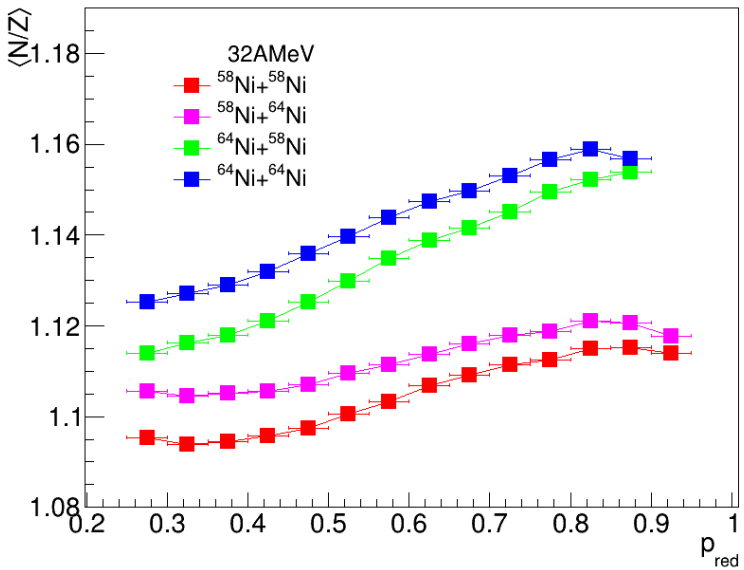

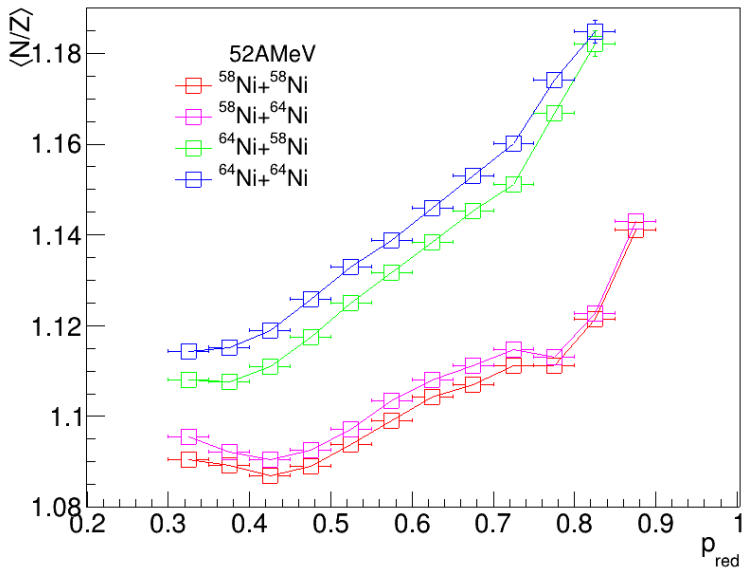

QP-QT isospin equilibration in mixed systems:

- visible in the $\langle N/Z \rangle$ of the QP vs p_{red}

Isospin equilibration

QPr channel

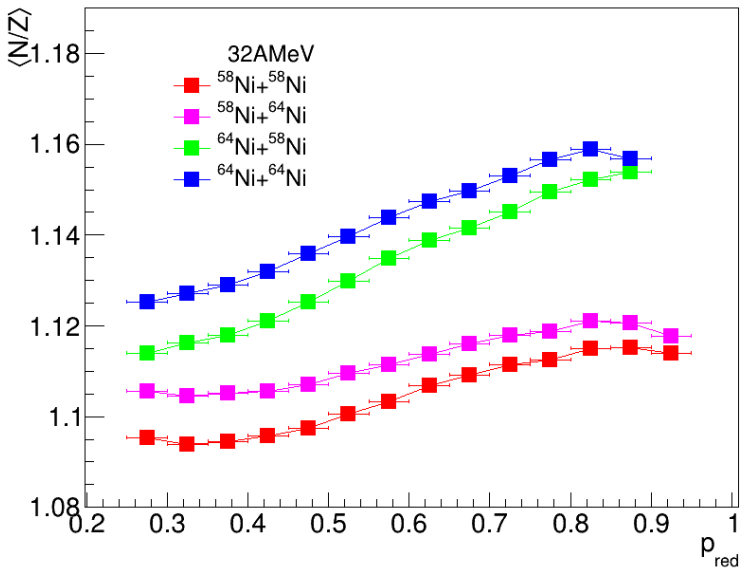

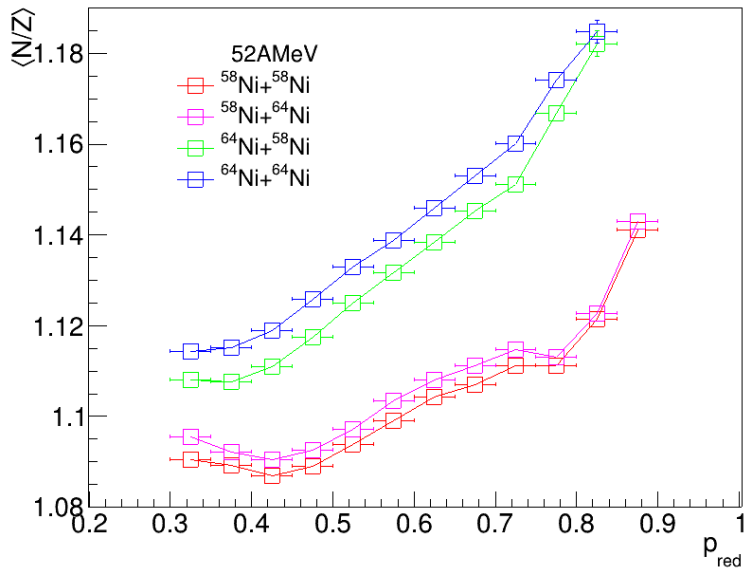

QP-QT isospin equilibration in mixed systems:

- visible in the $\langle \mathbf{N/Z} \rangle$ of the QP vs $\mathbf{p_{red}}$
- can be highlighted by using the **isospin transport ratio**: [09tsa, 21cam]

$$R = \frac{2X_{AB} - X_{AA} - X_{BB}}{X_{AA} - X_{BB}}$$

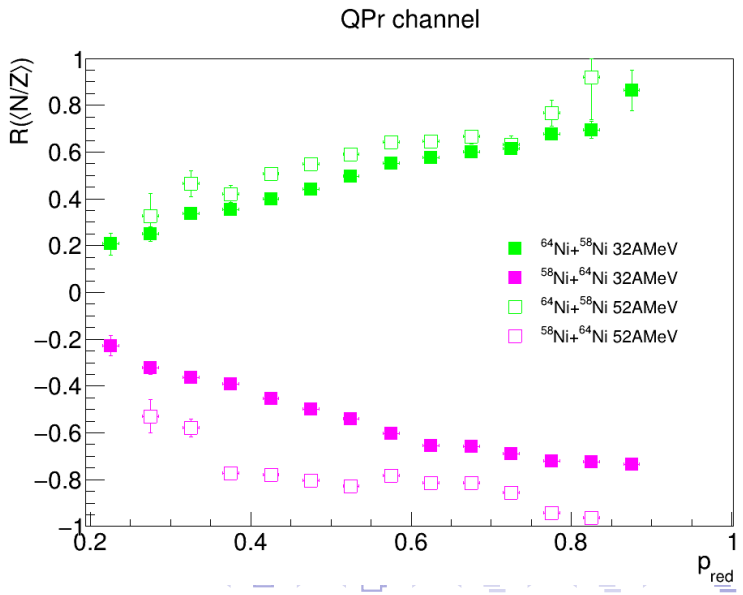

Isospin equilibration

QPb channel

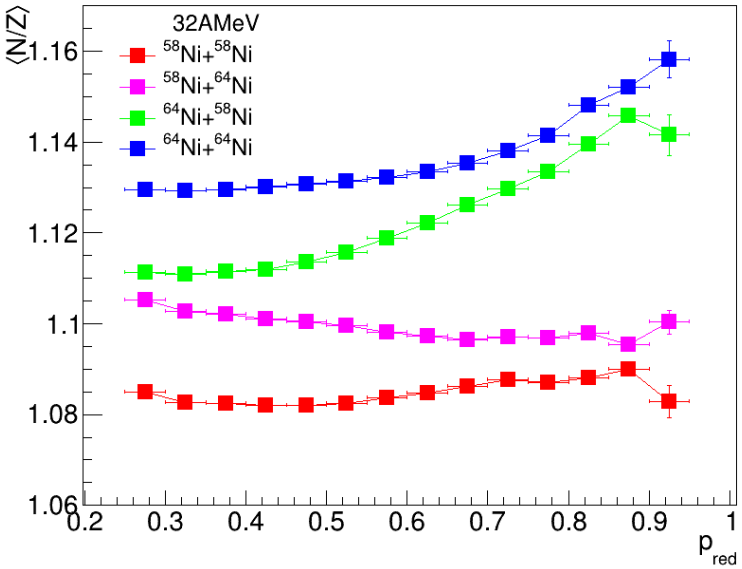

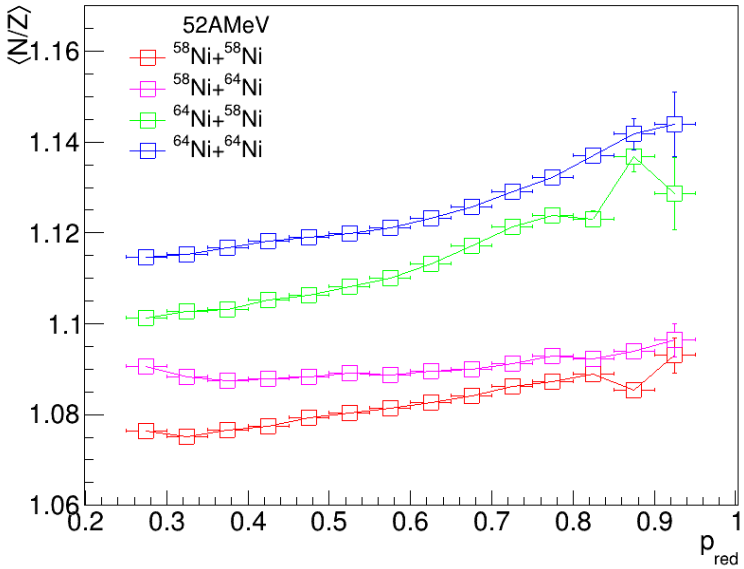

The isospin equilibration is clearly visible also from the characteristics of the QP reconstructed from the two breakup fragments in the QPb channel:
$\rightarrow R(\langle N/Z \rangle)$ vs $\mathbf{p_{red}}$

Isospin equilibration

QPb channel

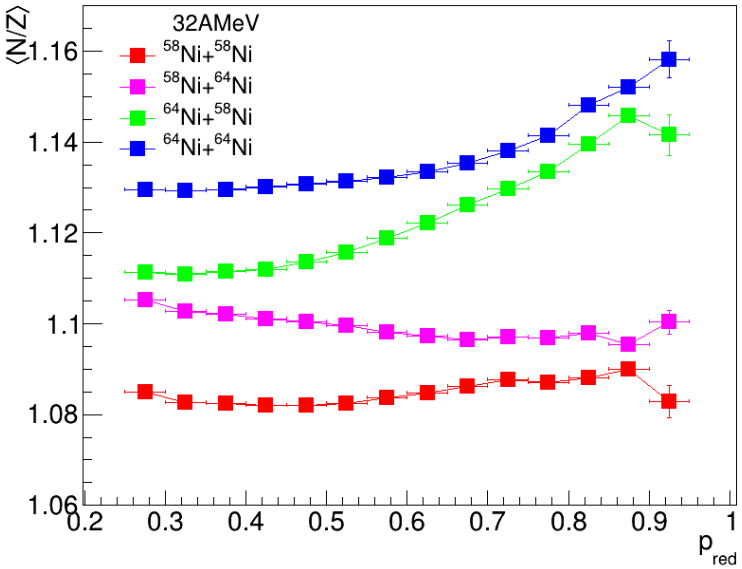

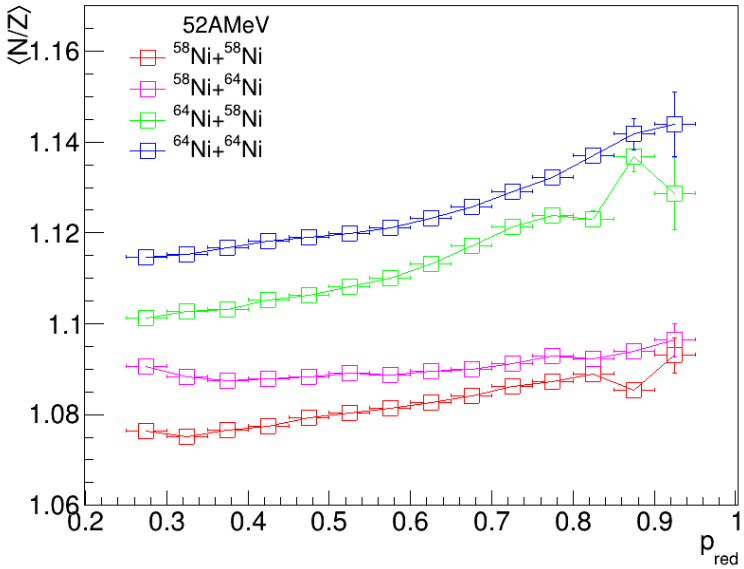

The isospin equilibration is clearly visible also from the characteristics of the QP reconstructed from the two breakup fragments in the QPb channel:
$\rightarrow R(\langle N/Z \rangle)$ vs $\mathbf{p_{red}}$

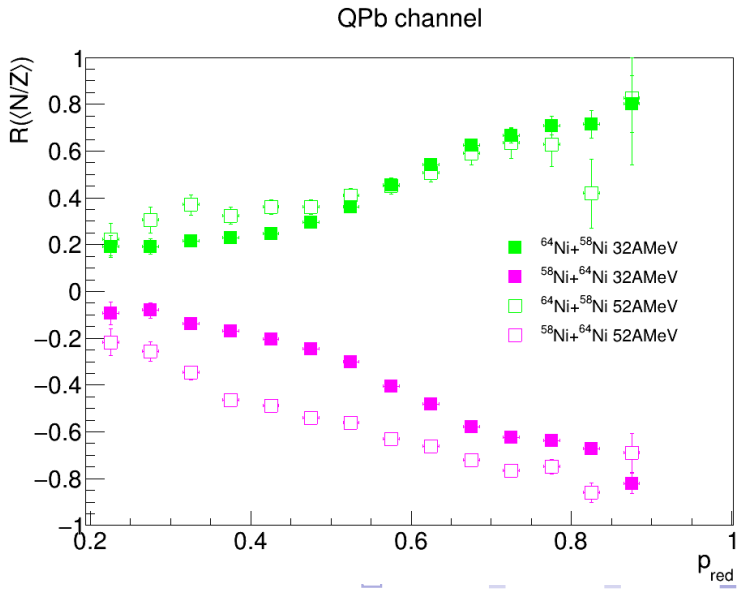

Isospin equilibration

Comparison between the QPr and QPb channels

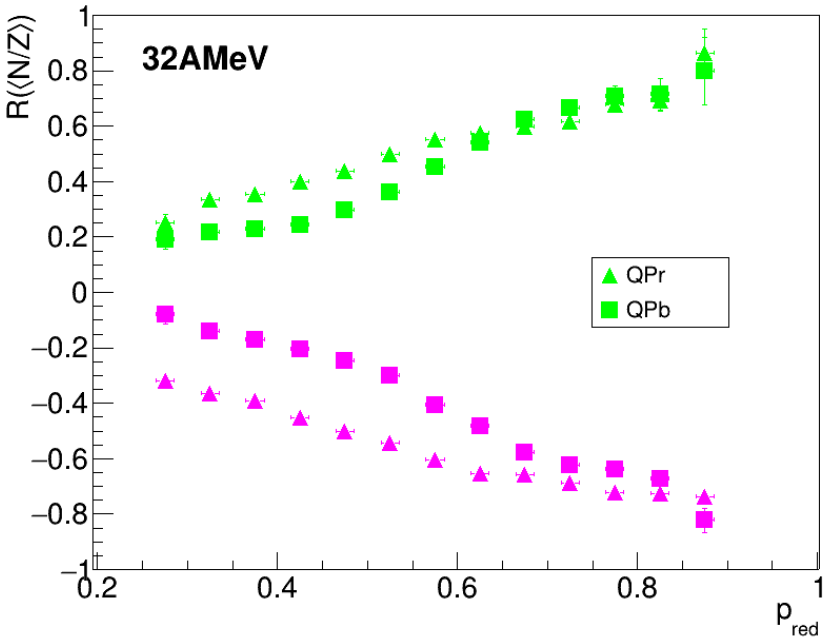

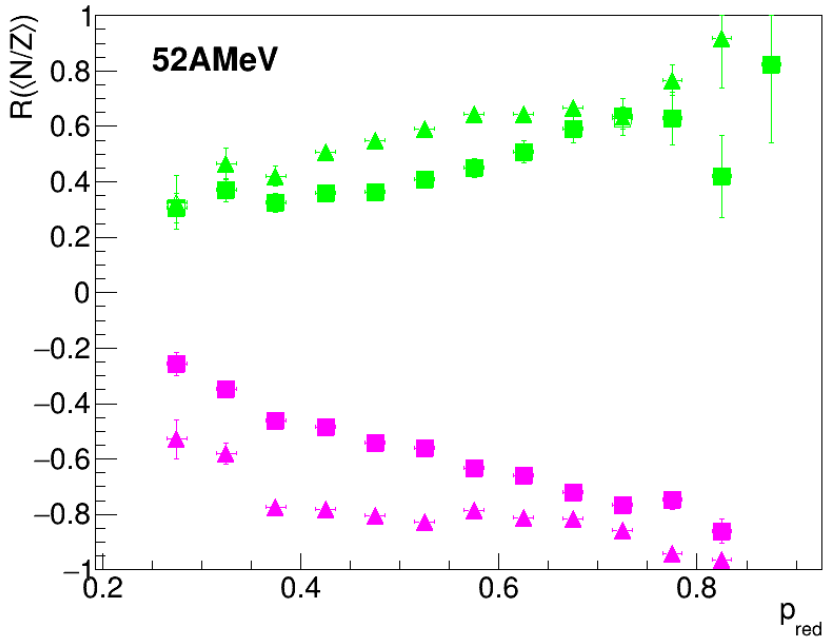

- We can compare the isospin equilibration phenomenon between the two selected reaction channels
- At both energies, for the same p_{red} value ($\Longrightarrow$ same reaction centrality) a higher degree of isospin equilibration is obtained for the QP reconstructed from the two breakup fragments in the QPb channel with respect to that obtained in the QPr channel.

Summary and future perspectives

Summary:

- INDRA-FAZIA E789 experiment: ^{64,58}Ni+^{64,58}Ni at 32 AMeV and 52 AMeV
- Selection of QP evaporation and QP breakup channels
- We studied the phenomenon of the QP-QT isospin equilibration in the two reaction channels: a stronger equilibration has been found in the QP breakup channel with respect to the QP evaporation channel.

Future perspectives:

- These results are preliminary: the data analysis is still in progress
- Further investigations on the isospin transport ratio:
  - studied as a function of other centrality related observables
  - calculated exploiting other isospin related observables
- Study of the isospin of the two QP breakup fragments H, L
- Detailed comparison between experimental data and model predictions, in order to obtain informations on the symmetry energy term of the NEoS:
  - Dynamical code: AMD
  - Statistical code: GEMINI, with comparisons among different afterburners [19pia]

References

[95pou] J. Pouthas et al., Nucl. Instr. and Meth. in Phys. Res. A 357, 418 (1995)

[14bou] R. Bougault et al., Eur. Phys. J. A 50, 47 (2014) *and references therein*

[19val] S. Valdré et al., Nucl. Instr. and Meth. in Phys. Res. A 930, 27 (2019) *and references therein*

[13li] B. A. Li et al., Phys. Lett. B 727, 276 (2013)

[21ree] B. T. Reed et al., Phys. Rev. Lett. 126, 172503 (2021)

[17rod] A. Rodriguez Manso et al., Phys. Rev. C 95, 044604 (2017)

[95ste] A.A. Stefanini et al., Z. Phys. A 351, 167 (1995)

[93cas] G. Casini et al., Phys. Rev. Lett. 71, 2567 (1993)

[00boc] F. Bocage et al., Nucl. Phys. A 676, 391 (2000)

[20pia] S. Piantelli et al., Phys. Rev. C 101, 034613 (2020)

[17jed] A. Jedele et al., Phys. Rev. Lett. 118, 062501 (2017)

[09tsa] M. B. Tsang et al., Phys. Rev. Lett. 102, 122701 (2009)

[21cam] A. Camaiani et al., Phys. Rev. C 103, 014605 (2021)

[19pia] S. Piantelli et al., Phys. Rev. C 99, 064616 (2019)

Backup slides

Nuclear Equation of State (NEoS)

Asymmetric nuclear matter

- We can separate the symmetric and the asymmetric term of the NEoS:

$$\frac{E}{A}(\rho,\delta) = \frac{E}{A}(\rho) + \frac{E_{sym}}{A}(\rho)\delta^2$$

  - 1^{st} *term*: binding energy for symmetric nuclear matter
  - 2^{nd} *term*: includes all the dependence from isospin asymmetry. Can be expanded around $\rho \sim \rho_0$:

$$\frac{E_{sym}}{A}(\rho) = J_{sym} + L_{sym}\left(\frac{\rho-\rho_0}{3\rho_0}\right) + \frac{1}{2}K_{sym}\left(\frac{\rho-\rho_0}{3\rho_0}\right)^2 + \dots$$

- $J_{sym} \sim 30$ MeV is the symmetry energy at $\rho = \rho_0$
- L_{sym} is the slope and K_{sym} the curvature (isovector incompressibility) of the asymmetric term, *not known with precision* (K_{sym} particularly)
- Theoretical models $\rightarrow$ two possible NEoS parametrisations: **asy-stiff** and **asy-soft**.
- Many efforts have been made in order to narrow down the uncertainty on the estimation for the NEoS parameters.

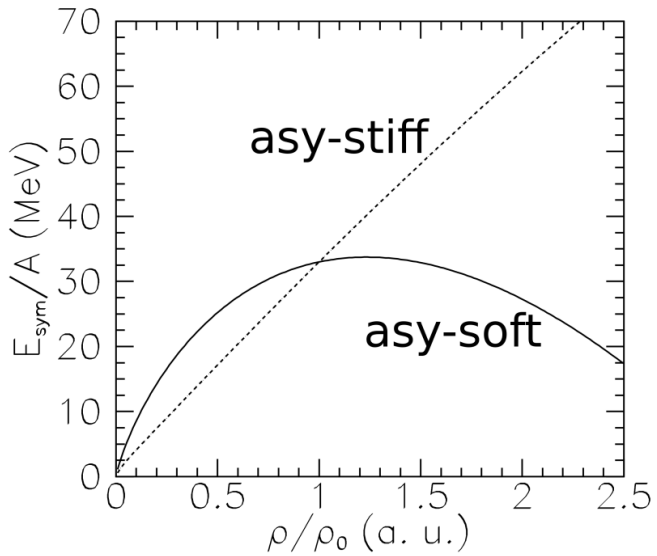

Nuclear Equation of State (NEoS)

Symmetry energy parameters

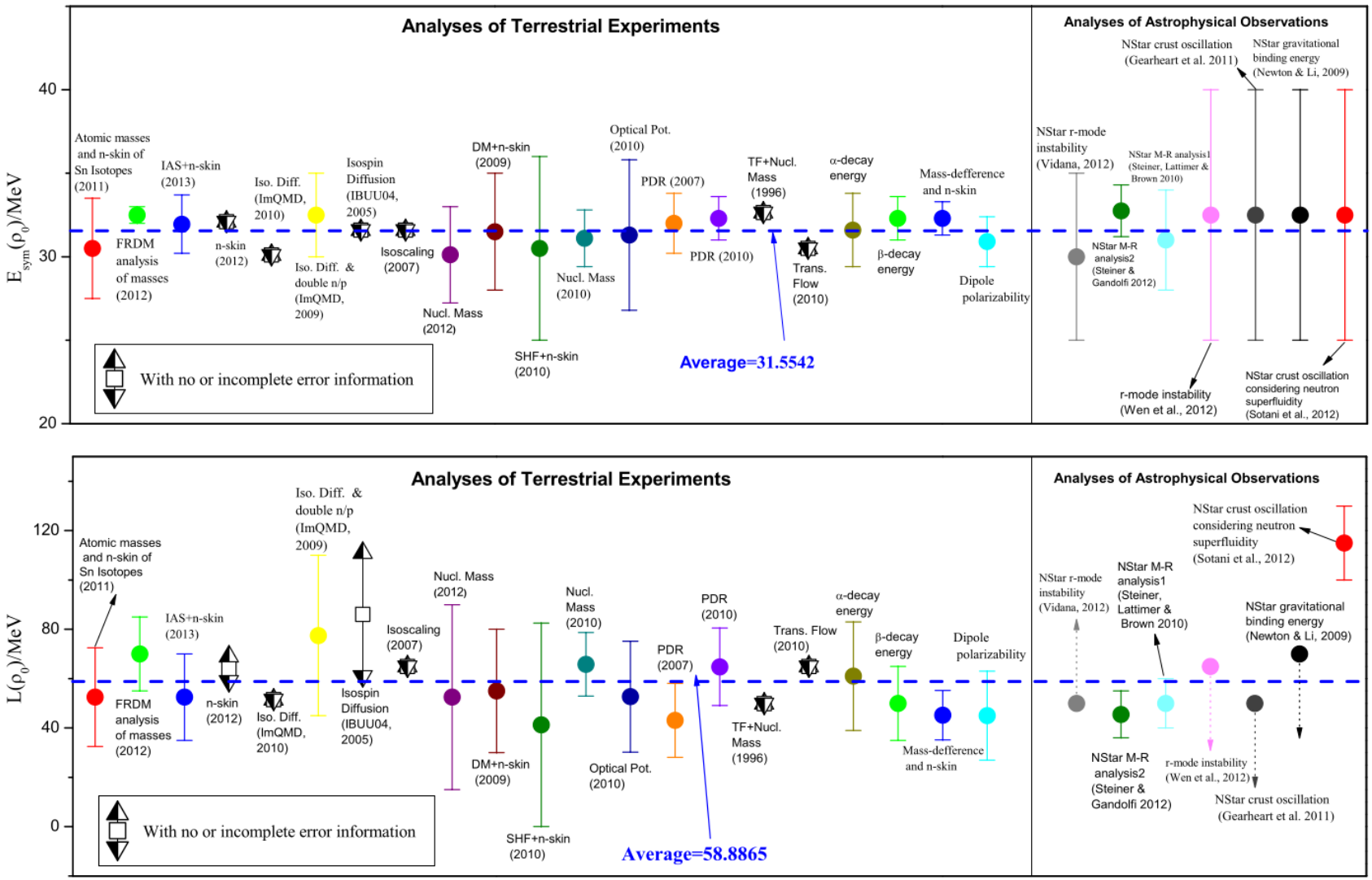

Fig. 1. (Color online.) Nuclear symmetry energy (upper) and its slope L (lower) at normal density of nuclear matter from 28 analyses of terrestrial nuclear laboratory experiments and astrophysical observations.

B. A. Li et al., Phys. Lett. B 727, 276 (2013)

Nuclear Equation of State (NEoS)

Symmetry energy parameters: some latest news

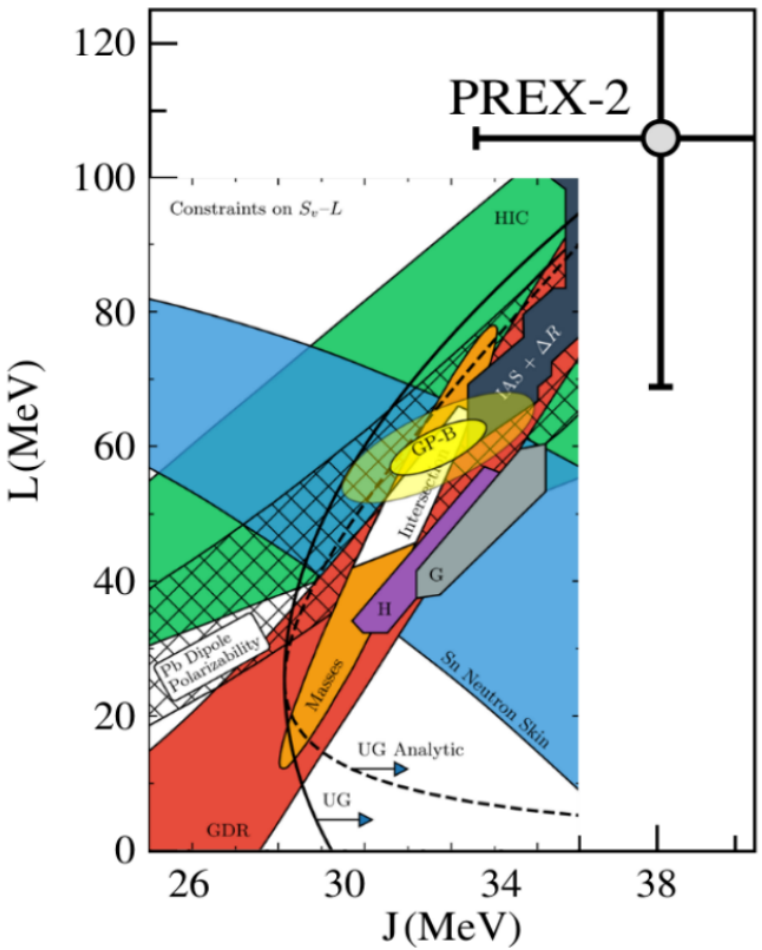

FIG. 2. Constraints on the J-L correlation obtained from a variety of experimental and theoretical approaches. The figure was adapted from Refs. [20,33] and noticeably displays the tension with the recent PREX-2 result.

B.T. Reed et al., PRL 126, 172503 (2021)

PREX-2 measurement of the neutron skin thickness of ^{208}Pb **(2021)**, which is correlated to the the slope of the symmetry energy:

$$R_{skin} = R_n - R_p = (0.283 \pm 0.071)\,\text{fm}$$

$$\downarrow$$

$$J_{sym} = (38.1 \pm 4.7)\,\text{MeV}$$
$$L_{sym} = (106 \pm 37)\,\text{MeV}$$

The result is considerably different from the current understanding of the NEoS.

Nuclear Equation of State (NEoS)

Isospin transport phenomena

- During peripheral and semiperipheral collisions, the symmetry energy term governs the **isospin transport phenomena**, i.e. the nucleon exchange between projectile and target
- It can be expressed as the difference between the neutron and proton currents between the two nuclei during the collision:

$$\mathbf{j}_n - \mathbf{j}_p \propto \frac{E_{sym}}{A}(\rho)\nabla\delta + \delta\frac{\partial\frac{E_{sym}}{A}(\rho)}{\partial\rho}\nabla\rho$$

We expect to see the effects of two contributions on the isospin related observables:

- **isospin diffusion**: driven by the presence of an isospin gradient in the system (asymmetric systems), leading to the isospin equilibration.
  Sensitive to $E_{sym}(\rho)/A$ $\rightarrow$ QP-QT isospin equilibration
- **isospin drift** (or *isospin migration*): associated to the presence of a density gradient (e.g. neck, where $\rho \lesssim \rho_0$). Can be isolated by choosing a symmetric system.
  Sensitive to $\frac{\partial E_{sym}(\rho)/A}{\partial\rho}$. $\rightarrow$ neutron enrichment of the neck region